Original Article

Whole blood viscosity modeling using power law, Casson, and Carreau Yasuda models integrated with image scanning U-tube viscometer technique

Yotsakorn Pratumwal[1], Wiroj Limtrakarn[2*], Sombat Muengtaweepongsa[3], Phatsawadee Phakdeesan[1], Suttirak Duangburong[2], Patipath Eiamaram[4], and Kannakorn Intharakham[3]

[1] Medical Engineering Program, Faculty of Engineering,
Thammasat University, Khlong Luang, Pathum Thani, 12120 Thailand

[2] Department of Mechanical Engineering, Faculty of Engineering,
Thammasat University, Khlong Luang, Pathum Thani, 12120 Thailand

[3] Department of Neuro, Faculty of Medicine, Thammasat University,
Khlong Luang, Pathum Thani, 12120 Thailand

[4] Design and Engineering Consulting Service Center, National Science and Technology Development Agency,
Ministry of Science and Technology, Khlong Luang, Pathum Thani, 12120 Thailand

Abstract

This study presented the image scanning U-tube viscometer technique to measure the whole blood viscosity. Two different constitutive models, power law and Casson, were selected to calculate blood viscosity. Results were compared with rotating viscometer. They had a good agreement at higher shear rates. Three constitutive models power law, Casson and Carreau Yasuda models were applied to blood viscosity data and used to simulate transient blood height in the U-tube. Comparison of the U-tube simulation and the actual experiment showed that Carreau Yasuda model is the most accurate model for whole blood viscosity measurement.

Keywords: U-tube viscometer, blood, viscosity, image processing, shear rate

1. Introduction

Blood viscosity is one of the most essential hemo-dynamic parameters which can establish the flow system of whole blood in vessels. Alteration in the blood viscosity leads to a two-fold opposite change in blood flow (Chen *et al.*, 2006). Many physiologic factors contribute to elevated whole blood viscosity including male gender, obesity, high

* Corresponding author.
  Email address: limwiroj@engr.tu.ac.th

sodium intake, aging and African race (Dormandy, 1970). Elevated whole blood viscosity leads to rapid growth of atherothrombotic lesions and augmented rate of plaque rupture (Simone *et al.*, 1990).

In fact, blood is a non-Newtonian fluid (Jung *et al.*, 2013; Kanaris *et al.*, 2006). Therefore, its viscosity changes the whole shear rate at the same location of artery in any time. The viscosity always changes because of pulse wave velocity from cardiac systole and diastole. The viscosity of blood becomes high when its shear rate is low as a result of cardiac diastole. On the contrary, the viscosity is low as the shear rate is high. Generally, no tool in any clinic can measure

the viscosity's whole shear rate. Rotating viscometer measures blood viscosity only a shear rates a time and not at low shear rate. As blood will coagulate after having been taken out from artery for more than three minutes, this creates the limit of time in blood viscosity measurement with the rotating viscometer (RV) (Baskurt *et al.*, 2009).

Scanning capillary tube viscometer (SCTV) was developed in order to measure the viscosity of the whole blood shear rate using the flow through the capillary tube. Power law model was selected to calculate the correlation of viscosity and shear rate (Kim *et al.*, 2000). Results from the SCTV were in accordance with RV at high shear rate. On the other hand, at the lowest shear rate, results from each method were different which meant the condition was affected with rheological yield stress (Kim, 2002). As a result, the viscosity of whole blood shear rate could not be illustrated with power law model. Casson model (Jung *et al.*, 2014) was developed after that to simplify the viscosity of whole blood shear rate with the yield stress. Then HB model was also implemented to describe the rheological yield stress (Kim *et al.*, 2009). Light transmission slit rheometer (LTSR) was selected to measure blood viscosity (Sehyun *et al.*, 2005). Red blood cell was studied with laser light. The laser's pressure and intensity according to time were used to calculate the aggregation index and viscosity. Pressure-scanning microfluidic hemo-rheometer developed using Casson and HB model showed excellent agreement with reference value (Lee *et al.*, 2011). However, Casson model showed better agreement with reference value than HB model.

Nowadays, image processing technique is applied worldwide. Blob detection is one of the techniques in image processing methods (Rosenfeld *et al.*, 1998). It uses mathematical methods that detect object regions in a digital image that are different in properties of brightness or color. Blob detection is used to obtain regions of interest for further processing such as histogram analysis to select varying levels of blood in U-tube.

This research showed the blood viscosity using U-tube and blood flow movement with image processing technique. Two models,p law and Casson, were used to calculate the relationship between viscosity and shear rate. The blood viscosity from the calculation was used in three models, power law, Casson and Carreau Yasuda (Fung, 2013). Results showed the accuracy of rheological models in blood behavior detection, and the blood viscosity will be used to calculate the blood flow past the carotid bifurcation in stroke patients (Pratumwal *et al.*, 2014).

2. Materials and Methods

2.1 Description of instruments

Image scanning U-tube viscometer schematic diagram is shown in Figure 1. There is a U-Tube, three ways for direction change of blood flow, a ruler scale and a marker for blood level calibration in image processing program and a D700 cannon camera for blood flow record. The U-tube's inner diameter was 2.4 mm. The distance from the top to bottom of the marker was 70 mm. There was also an air heater to control blood temperature at 37°C which is normal human body temperature.

As image processing program which can be run on window was developed to determine the level of the blood that changed through time in U-tube as shown in Figure 2. The moving zone of blood is detected and the brightness and color of digital are used to obtain the height of blood change. The video files from the camera were analyzed with this program to show results in the relationship between the level of blood in U-tube and time. These results were the input data for the viscosity of blood whole shear rate calculation. The advantage of image scanning U-tube viscometer is that it requires only 2 cm^3 of blood sample. Each sample was tested for two minutes. Blood level change in U-tube was recorded into video files with 50 frames per second to detect $h_1(t)$ and $h_2(t)$ level change of blood flow in U-tube.

2.2 Testing procedure

First, turn on the video camera, computer and air heater. After that, inject blood into the U-tube via inlet fluid channel; try to make $h_1(t)$ higher than $h_2(t)$, with both of the levels between the top and bottom of the image marker. Another blood sample was transferred to a test cup of rotating viscometer (Brookfield model DV-II, spindle SC4-21, sample volume 8 cm^3, viscosity range 0.025-0.5 Pa.s and lower shear rate limit 9.3 sec^{-1}) to measure its viscosity to compare with the viscosity derived from the image scanning U-tube viscometer.

Then connect three-way valves with the left and right side of the U-tube. At this stage, the blood would find its equilibrium within 1 minute and 30 seconds. A video file was recorded by a digital camera, analyzed with the image processing program which was developed for this experiment. The results from the program were in pixels position
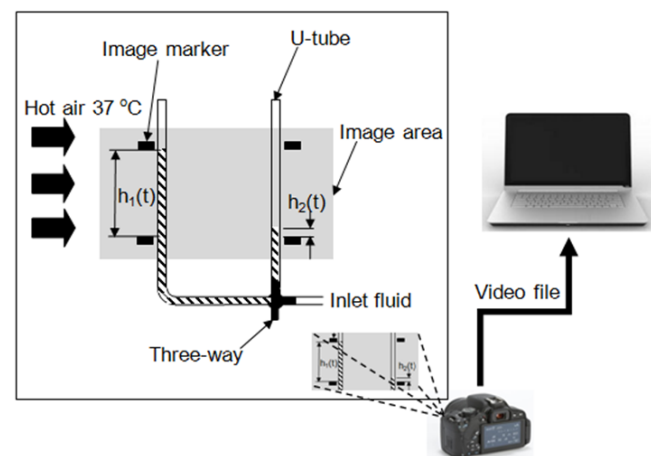

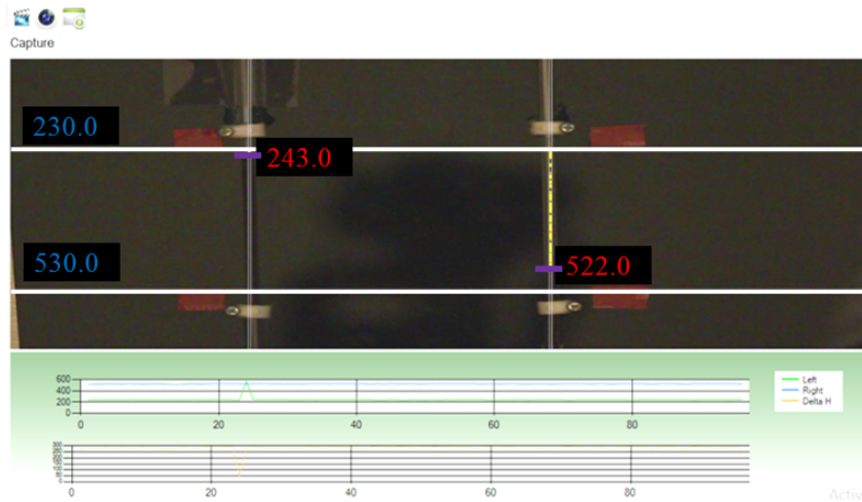Figure 1. Schematic diagram of image scanning U-tube viscometer.

Figure 2.   Image processing program was developed to determine the level of the blood.

according to time and converted to $h_1(t)$ and $h_2(t)$ as shown in Figure 3. These data were computed for blood viscosity.

2.3 Data analysis

2.3.1 Blood flow analysis

Blood in U-tube shown in Figure 1 had different levels. Before the experiment, one side of the U-tube's walls was dry while another was wet. At this point, the effect of surface tension and yield stress of blood appeared when its level changed to find equilibrium as a result of gravity. This could be a reason why the levels of the two sides of the U-tube were not the same.

Conservation of energy was included in the mathematical model that illustrated the flow behavior in the U-tube. The assumptions were the quasi-steady flow and the

constant of surface tension for the liquid-solid surface. The governing equation is as follows (Jung *et al.*, 2014).

$$P_1 + \frac{1}{2}\rho V_1^2 + \rho g h_1(t) = P_2 + \frac{1}{2}\rho V_2^2 + \rho g h_2(t) + \Delta P(t) + \rho g \Delta h_{st}$$

(1)

where P_1 and P_2 are the static pressure on each side of U-tube, g is gravity acceleration, Δh_{st} is the distance of height from surface tension, $\Delta P(t)$ is the pressure drop across U-tube, ρ is density of blood, V_1 and V_2 is blood velocity at each side of U-tube. Pressure drop across U-tube and forms $P_1 = P_2 = P_{atm}$ and $|V|_1 = |V|_2$

$$\Delta P(t) = \rho g \left[h_1(t) - h_2(t) - \Delta h_{st} \right]$$

(2)

2.3.2 Mathematical procedure with constitutive models

The power law and Casson Model were selected to calculate the viscosity, power-law model is a simple constitutive model that shows good description of fluid behavior across the range of shear rates to which the coefficients were fitted while Casson model also considers yield stress in term of blood viscosity.

1) Power law model

Power law is a non-Newtonian fluid model that does not consider the yield stress. The relationship between viscosity and shear rate of power-law model can be written as follows

$$\eta = m\dot{\gamma}^{n-1}$$

(3)

where η is the apparent viscosity, $\dot{\gamma}$ is the shear rate, m and n are the power-law constants model which are derived from fitting curve from image scanning U-tube viscometer.

Hagen-Poiseuille flow provides relationship for the pressure drop, flow rate and blood viscosity. For non-
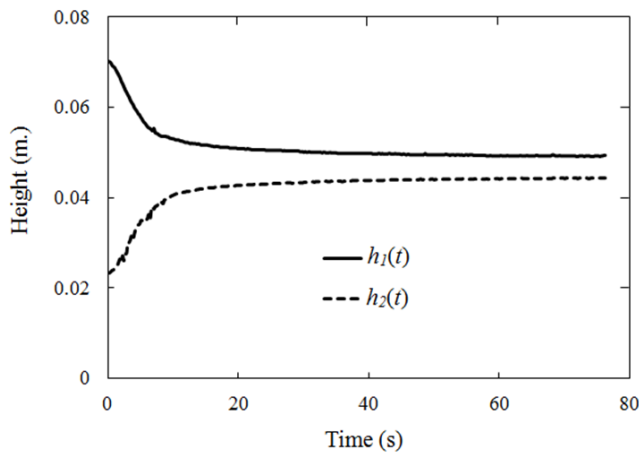

Figure 3. $h_1(t)$ and $h_2(t)$ according to time.

Newtonian fluids, viscosity changes with shear rate when applied with power law model to above relation that satisfies for Newtonian fluid. The pressure drop can be written as follows (Kim *et al.*, 2002).

$$\Delta P(t) = \frac{2\eta L\dot{\gamma}}{R} = \frac{2mL\dot{\gamma}^n}{R} \tag{4}$$

$$= \frac{2mL}{R}\left\{\left(\frac{3n+1}{n}\right)\frac{Q}{\pi R^3}\right\}^n$$

$$= \frac{2mL}{R}\left\{\left(\frac{3n+1}{n}\right)\frac{1}{R}\left|\frac{dh}{dt}\right|\right\}^n$$

where L and R are length and radius of U-tube, respectively while $\dot{\gamma} = \left(\frac{3n+1}{n}\right)\frac{Q}{\pi R^3}$ and $Q = \pi R^2 |V_1| = \pi R^2 \left|\frac{dh}{dt}\right|$

For non-Newtonian power law calculation Equation 2 to 4 apply

$$\rho g\left[h_1(t) - h_2(t) - \Delta h_{st}\right] = \frac{2mL}{R}\left\{\left(\frac{3n+1}{n}\right)\frac{1}{R}\left|\frac{dh}{dt}\right|\right\}^n \tag{5}$$

Defining a new function $\theta(t) = h_1(t) - h_2(t) - \Delta h_{st}$ then substituting in Equation 5:

$$\frac{d\theta}{\theta^{\frac{1}{n}}} = -\beta dt \tag{6}$$

where $\beta = \dfrac{\left(\dfrac{\rho g R}{2mL}\right)^{\frac{1}{n}}}{\left(\dfrac{3n+1}{n}\right)\left(\dfrac{1}{2R}\right)}$

The above equation can be integrated as follows.

$$\theta(t) = \left\{\theta(0)^{\frac{n-1}{n}} - \left(\frac{n-1}{n}\right)\beta t\right\}^{\frac{n}{n-1}} \tag{7}$$

Equation 7 was used for curve fitting of the experimental data $h_1(t)$ and $h_2(t)$ to determine power Law index, n, and consistency index, m. MATLAB R2010a was used in the curve fitting. After that the shear rate and blood viscosity could be calculated as follows.

$$\dot{\gamma} = \left\{\frac{\rho g R}{2mL}\theta(t)\right\}^{\frac{1}{n}} \tag{8}$$

$$\eta = m\dot{\gamma}^{n-1} \tag{9}$$

2) Casson Model

Casson model is a shear thinning fluid with yield stress term that explains blood viscosity behavior and could be described with following equation.

$$\sqrt{\tau} = \sqrt{\tau_y} + \sqrt{k}\sqrt{\dot{\gamma}} \quad \text{when } \tau \geq \tau_y \tag{10}$$

$$\dot{\gamma} = 0 \quad \text{when } \tau < \tau_y \tag{11}$$

where τ_y is yield stress and k is a Casson model constant. The velocity profile in U-tube can be described using Casson model with integration of shear rate as follows.

$V(t,r) =$

$$\frac{R^2\Delta P(t)}{4kL}\left[1 - C^2(r) - \frac{8}{3}C_y^{\frac{1}{2}}(t)\left\{1 - C^{\frac{3}{2}}(r)\right\} + 2C_y(t)(1-C(r))\right]$$

for $r_y(t) \leq r \leq R$ (12a)

$$V(t,r) = \frac{R^2\Delta P(t)}{4kL}\left(1 - \sqrt{C_y(t)}\right)^3\left(1 + \frac{1}{3}\sqrt{C_y(t)}\right)$$

for $r_y(t) \geq r$ (12b)

where $C(r) = \dfrac{r}{R}$

and $C_y(t) = \dfrac{r_y(t)}{R} = \dfrac{\tau_y}{\tau_w(t)} = \dfrac{\Delta h_y}{h_1(t) - h_2(t) - \Delta h_{st}}$

Equation 12 was used for curve fitting of the experimental data $\left[d(h_1(t) - h_2(t))\right]/dt$ to determine the three unknowns, Δh_{st}, k and Δh_y using MATLAB R2010a. At this point, the shear rate and blood viscosity can be calculated as follows.

$$\dot{\gamma}_w(t) = \frac{\rho g R}{2kL}\left(\sqrt{h_1(t) - h_2(t) - \Delta h_{st}} - \sqrt{\Delta h_y}\right)^2 \tag{13}$$

$$\eta(t) = \frac{\rho g R\left[h_1(t) - h_2(t) - \Delta h_{st}\right]}{2\dot{\gamma}_w(t)L} \tag{14}$$

3. Results and Discussion

After measuring the blood levels in U-tube viscometer, with the image processing program and plotting height-versus-time graph as shown in Figure 3, the experimental data would be used to find blood viscosity from power law model in Equation 7 and the power law constant by curve fitting. The constant would be used to calculate the shear rate and blood viscosity in Equation 8 and 9, respectively. The results were plotted into graph shown in Figure 4. The viscosity at low shear rate was higher than at high shear rate.

As blood is a non-Newtonian fluid. The effect of red blood cell was in a chaotic flow in the first period as a result of its poor arrangement at high shear rate which made it more difficult to measure the viscosity.

For Casson model, its graph from the experiments was used to calculate the velocity according to $h_1(t) - h_2(t)$ in Figure 5. The graph was applied to curve fitting with Equation
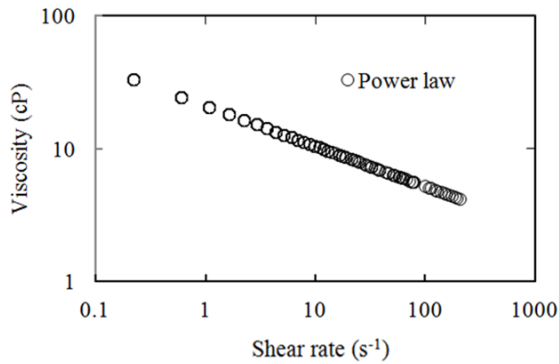
Figure 4. Relationship between viscosity and shear rate of blood from power law model.

12 to obtain the constant value. Then the constant would be used in Equation 13 and 14 to calculate the viscosity and shear rate of the blood as shown in Figure 6. When we compared the results from Casson and power law models, it showed that at low shear rate, the viscosity from Casson model was higher than power law because the Casson model considered yield stress of blood behavior while power law did not.

Figure 7 is the relationship between blood viscosity in whole shear rate from image scanning U-tube viscometer using power law, Casson model and rotating viscometer. Results from rotating viscometer and Casson model were in good agreement. While results from power law and rotating viscometer was not, but they had the same trend. This rotating viscometer can only measure viscosity at high shear rate and measure only a value at a time. So, the rotating viscometer has a limit as blood will coagulate after having been taken out from artery for more than three minutes.

Blood viscosity in the whole of shear rate is important for using the analysis of blood flow in the carotid artery. The results show the stress and the chance of plaque rupture (Pratumwal *et al.*, 2014). The result is used to diagnose the patients with atherosclerosis.

Studying the model of this non-Newtonian fluid showed the behavior of blood flow. Three models were selected to simulate the flow in U-tube. So, there were three simulations according to the three models. Firstly, results from power law model are shown in Figure 4, as the power law constant was derived from a following equation.

$$\eta = m\dot{\gamma}^{n-1} \tag{15}$$

Secondly, the graph in Figure 6 was calculated from the Casson model. The curve was fitted with the Casson model equation as follows.

$$\sqrt{\eta} = \sqrt{\frac{\tau_y}{\dot{\gamma}}} + \sqrt{K} \tag{16}$$

where K is a viscosity consistency. Thirdly, the curve from the Casson model in Figure 6 was fitted by the Carreau-Yasuda model equation as below.

$$\eta = \eta_{\infty} + \frac{\left(\eta_0 - \eta_{\infty}\right)}{\left(1 + \left(\lambda\dot{\gamma}\right)^a\right)^{\frac{1-n}{a}}} \tag{17}$$

where a is Yasuda exponent, n is power law index, λ is time constant, η_0 is viscosity at zero shear rate and η_{∞} is viscosity at infinite shear rate.

The viscosity from U-tube testing was applied to analyze blood flow in the U-tube by the three models. The
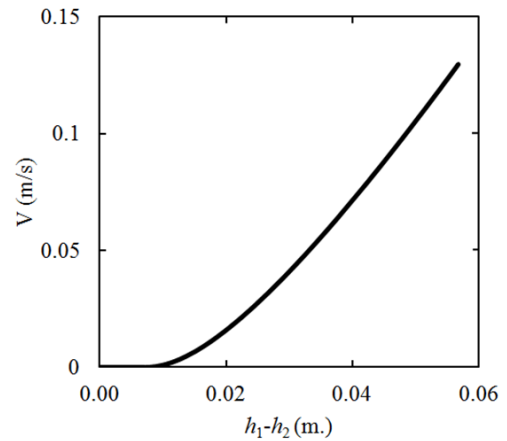

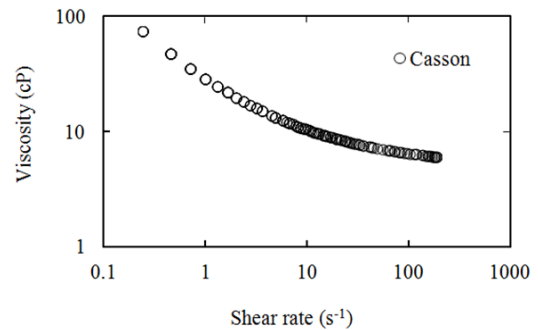Figure 5. Velocity according to $h_1(t) - h_2(t)$.

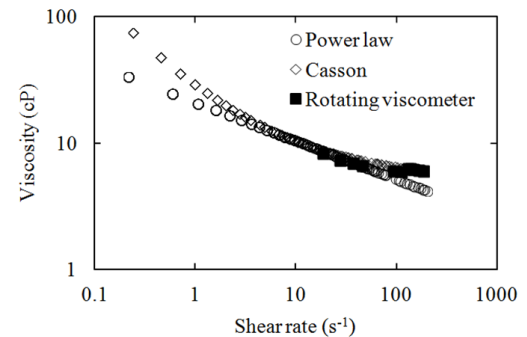Figure 6. Relationship between viscosity and blood shear rate from Casson model.

Figure 7. Viscosity and shear rate of blood using power law, Casson model and rotating viscometer.
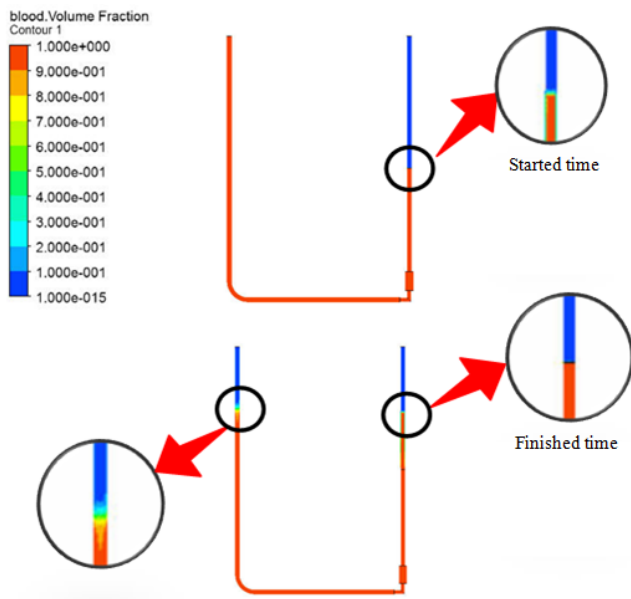
Figure 8. Blood level at started and the end of an experiment.

simulated conditions started from different blood levels (Figure 8) and then let blood flow under gravity. The flow simulation had transient problem from multiphase flow with blood and the air. The analysis used ANSYS CFX V.14. Results from these three models would be compared with the actual measurement from the image scanning U-tube viscometer.

Figure 9 compares the height of h_1 according to time of the blood flow under gravity from realistic condition, power law, Casson and Carreau Yasuda. It showed that the most precise results were from Carreau Yasuda model. With the information, Carreau Yasuda model could be the most suitable model for blood flow analysis (Gijsen *et al.*, 1999) and (Chen *et al.*, 2006).
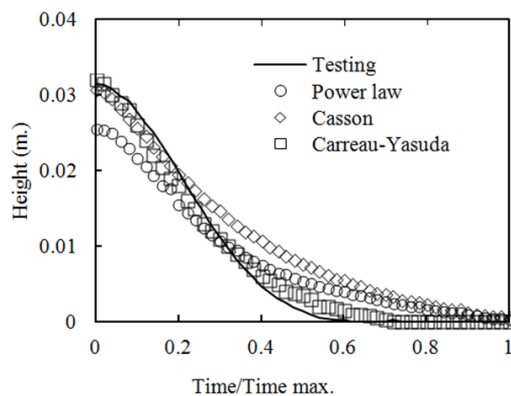

Figure 9. h_1 according to time from realistic conditions, power law, Casson and Carreau Yasuda model.

4. Conclusions

This research aims to develop a technique to measure a non-Newtonian blood viscosity by capturing the change of blood level in U-tube using image processing. Firstly, the relationship between viscosity and shear rate from the power law and Casson model were measured and compared to rotating viscometer. As a result, the Casson model was the closest to the results from the RV because Casson model could illustrate the behavior of blood which is a non-Newtonian fluid with yield stress as a result of poor red blood cells arrangement.

Secondly, the simulation of blood flow in the U-tube is analyzed. The results from the Carreau Yasuda model were the closet to the results from the image processing. For future work, we should measure the blood viscosity and the geometry of carotid bifurcation from MRI of stroke patients. This information is used to calculated blood flow in carotid bifurcation to predict the chance of plaque rupture in patients.

Acknowledgements

References

Baskurt, O. K., Boynard, M., Cokelet, G. C., Connes, P., Cooke, B. M., Forconi, S., . . . Wautier, J. L. (2009). International expert panel for standardization of hemorheological, New guide-lines for hemorheological laboratory techniques. *Clinical Hemorheology and Micro-circulation, 42*, 75-97.

Chen, J., & Li, Y. (2006). Coal fly ash as an amendment to container substrate for Spathiphyllum production. *Bioresource Technology, 97*(1), 1920-1926.

Chen, J., Lu, X. Y., & Wang, W. (2006). Non-Newtonian effects of blood flow on hemodynamics in distal vascular graft anas-tomoses. *Journal of Biomechanics, 39*, 1983-1995.

Cowan, A. Q., Cho, D. J., & Rosenson, R. S. (2012). Importance of blood rheology in the pathophysiology of athero-thrombosis. *Cardiovascular Drugs and Therapy, 26*, 339-348.

Dormandy, J. A. (1970). Clinical significance of blood viscosity. *Annals of the Royal College of Surgeons of England, 47*, 211-228.

Fung, Y. (2013). *Biomechanics: Motion, flow, stress, and growth*. Berlin, Germany: Springer Science & Business Media.

Gijsen, F., Allanic, E., Van de Vosse, F., & Janssen, J. (1999). The influence of the non-Newtonian properties of blood on the flow in large arteries: Unsteady flow in a 90 curved tube. *Journal of Biomechanics, 32*, 705-713.

Gijsen, F., Van de Vosse, F., & Janssen, J. (1999). The influence of the non-Newtonian properties of blood on the flow in large arteries: Steady flow in a carotid bifurcation model. *Journal of Biomechanics, 32*, 601-608.

Jung, J. M., Lee, D. H., & Cho, Y. I. (2013). Non-Newtonian standard viscosity fluids. *International Communications in Heat and Mass Transfer, 49*, 1-4.

Jung, J. M., Lee, D. H., Kim, K. T., Choi, M. S., Cho, Y. G., Lee, H. S., . . . Kim, D. S. (2014). Reference intervals for whole blood viscosity using the analytical performance-evaluated scanning capillary tube viscometer. *Clinical Bio-chemistry, 47*, 489-493.

Kanaris, A., Anastasiou, A., & Paras, S. (2012). Modeling the effect of blood viscosity on hemodynamic factors in a small bifurcat-ed artery. *Chemical Engineering Science, 71*, 202-211.

Kim, S. (2002). *A study of non-Newtonian viscosity and yield stress of blood in a scanning capillary-tube rheometer*. Philadelphia, PA: Drexel University.

Kim, S., Cho, Y. I., Hogenauer, W. N., & Kensey, K. R. (2002). A method of isolating surface tension and yield stress effects in a U-shaped scanning capillary-tube viscometer using a Casson model. *Journal of Non-Newtonian Fluid Mechanics, 103*, 205-219.

Kim, S., Cho, Y. I., Kensey, K. R., Pellizzari, R. O., & Stark, P. R. (2000). A scanning dual-capillary-tube viscometer. *Review of Scientific Instruments, 71*, 3188-3192.

Kim, S., Namgung, B., Ong, P. K., Cho, Y. I., Chun, K. J., & Lim, D. (2009). Determination of rheological properties of whole blood with a scanning capillary-tube rheometer using constitutive models. *Journal of Mechanical Science and Technology, 23*, 1718-1726.

Lee, B. - K., Xue, S., Nam, J., Lim, H., & Shin, S. (2011). Determination of the blood viscosity and yield stress with a pressure-scanning capillary hemorheometer using constitutive models. *Korea-Australia Rheology Journal, 23*, 1-6.

Pratumwal, Y., Limtrakarn, W., & Premvaranon, P. (2014). The analysis of blood flow past carotid bifurcation by using the one-way fluid solid interaction technique (FSI). *Journal of Research and Applications in Mechanical Engineering, 2*, 57-64.

Rosenfeld, A., & Chiao-Yung, S. (1998). Detecting image primitives using feature pyramids. *Information Sciences, 107*, 127-147.

Sehyun, S., Myung - Su, P., Yunhee, K., Joo-Hee, J., & Jang - Soo, S. (2005). Simultaneous measurement of red blood cell aggregation and viscosity: Light transmission slit rheometer. *Journal of Mechanical Science and Technology, 19*, 209-215.

Simone, G. de, Devereux, R. B., Chien, S., Alder-man, M. H., Atlas, S. A., & Laragh, J. H. (1990). Relation of blood viscosity to demographic and physiologic variables and to cardiovascular risk factors in apparently normal adults. *Circulation, 81*, 107-117.